Biointerface Research in Applied Chemistry
Platinum Open Access Journal (ISSN: 2069-5837)

Article
Volume 11, Issue 4, 2021, 11891 - 11904
https://doi.org/10.33263/BRIAC114.1189111904

Adsorption Study of Cu^{2+} Ions from Aqueous Solutions by Bael Flowers (*Aegle marmelos*)

Shakila H. Peli Thanthri [1], Kavitha H. Ranaweera [1], Bupani Asiri Perera [1,*]

[1] Department of Chemistry, University of Sri Jayewardenepura, Gangodawila, Nugegoda, Zip Code: 10250, Western Province, Sri Lanka
* Correspondence: basirip@sjp.ac.lk;

Scopus Author ID 7005616983
Received: 2.10.2020; Revised: 15.12.2020; Accepted: 17.12.2020; Published: 20.12.2020

Abstract: In the present study, batch mode adsorption was carried out to investigate the adsorption capacity of dried bael flowers (*Aegle marmelos*) for the adsorptive removal of Cu(II) ions from aqueous solutions by varying agitation time, initial metal concentration, the dose of adsorbent, temperature, and initial pH of the Cu(II) ion solution. The percentage removal of 98.7% was observed at 50 ppm initial metal ion concentration, 0.5 g/100.00 cm^3 adsorbent dosage, within the contact time of 120 minutes at 30 ºC in the pH range of 4 – 7. The sorption processes of Cu(II) ions was best described by pseudo-second-order kinetics. Langmuir isotherm had a good fit with the experimental data with 0.97 of correlation coefficient (R^2), and the maximum adsorption capacity obtained was 23.14 mg g^{-1} at 30 ºC. The results obtained from sorption thermodynamic studies suggested that the adsorption process is exothermic and spontaneous. SEM analysis showed tubular voids on the adsorbent. FTIR studies indicated the presence of functional groups like hydroxyl, –C-O, –C=O, and amide groups in the adsorbent, which can probably involve in metal ion adsorption. Therefore, dried bael flowers can be considered an effective low-cost adsorbent for treating Cu(II) ions.

Keywords: dried bael flowers; adsorption; isotherms; kinetics; copper (II).

1. Introduction

Water pollution has become a severe and considerable problem throughout the world, mainly because the percentage of consumable freshwater is limited. Contamination of water by toxic heavy metals related to industrial wastewater discharge has become a considerable environmental problem worldwide. Those are irreplaceable from industries due to their high value [1].

Copper is an essential trace metal for living beings as it is required as a catalyst for many enzymes [2]. Yet, high levels of copper can be extremely toxic and can lead to serious health problems. Copper tends to accumulate in the liver upon excessive ingestion and cause kidney problems, anemia, and gastrointestinal problems [3]. Electroplating industries, petroleum refining, mining, brass manufacture, and Cu-based agriculture are a few examples of the industries that use copper [3]. The permissible limit of copper for industrial effluents discharge into the water bodies is 0.25 mg/L, according to the U.S. Environmental Protection Agency Standards [4]. However, pollution of natural water bodies due to copper contamination has been reported from several countries such as Bangladesh [5] and Turkey [6], emphasizing the importance of investigating the cost-effective methods to remove these contaminants from aqueous solutions.

Many modern, cost-effective methods are being experimented with throughout the world for heavy metal removal, including electro spark method [7], electrocoagulation [8], coagulation-flocculation [9], Photocatalysis [10], ion exchange [11], and membrane filtration [12]. Compared with other methods, the adsorption process has gained more interest as a more promising, long-term method. It seems to be a more effective and economical approach for heavy metal removal due to its less capital cost, minimal use of chemicals, and easy operation [13].

Various adsorbents have been researched for their potential for the adsorptive removal of heavy metals, including groundnut shell [14], organic waste [15], Clearing nut seed powder [16], residue powder of *Padina gymnospora* [17], Pistachio shell [18], Soya Bean [19], and Persimmon leaf [20]. However, no reported studies are based on bael flowers used as an alternative adsorbent for heavy metal removal.

Bael *(Aegle marmelos)* is a medium-sized, armed, deciduous tree that belongs to the Rutaceae family [21]. Bael tree is mostly used in Ayurvedic medicine. Hot water extract of dried bael flower can treat dysentery, diarrhea, and vomiting [22]. Residue remains after extracting hot water extract of bael flowers is not used for any purpose, but disposed of as waste. Herein, we explore the potential of bael flowers (*Aegle marmelos*) as a novel adsorbent to remove the Cu(II) ions from aqueous solutions. Operating parameters effect for the adsorption process such as solution pH, initial metal concentration, agitation time, adsorbent dosage, and temperature were investigated regarding the removal of Cu(II) ions, which is present toxic contaminant in many industrial effluents.

2. Materials and Methods

2.1. Preparation of the adsorbent.

Bael (*Aegle marmelos*) flowers collected from the local market were washed with tap water to remove dust particles and impurities. Flowers were dried under sunlight and ground to reduce the particle size and sieved to obtain a 250-500 µm uniform sample. Ground bael flowers were washed with deionized water to remove surface impurities and then washed with hot deionized water (70 ºC) to remove soluble colored components. The sample was dried at 70 ºC for 3 hours in an oven and stored in sealed plastic bags. The obtained dried bael flowers (DBF) were used as the adsorbent throughout the adsorption experiment.

2.2. Characterization of dried bael flowers.

FTIR analysis was performed with a Thermo Fisher SCIENTIFIC NICOLET iS10 IR spectrometer with a spectral range 4000-400 cm^{-1} to identify the functional groups present on DBF examine the changes before and after the adsorption process.
To analyze the surface morphology of the adsorbent SEM analysis was carried out with SU6600 microscope with an acceleration voltage of 15.0 kV.

2.3. Preparation of the adsorbate.

Stock solutions of 1000 ppm Cu(II) were prepared in 1000 cm^3 volumetric flasks by dissolving 3.8547 g of $Cu(NO_3)_2.3H_2O$ (Breckland Scientific Suppliers) using distilled water. Test solutions were prepared by diluting the stock solutions. 0.1M NaOH and 0.1M HNO_3 solutions were used to adjust the test metal ion solutions' pH.

2.4. Batch adsorption studies.

Batch adsorption studies were done to investigate the effects of factors on the adsorption process (contact time, initial metal concentration, adsorbent dosage, temperature, and pH). To perform the batch adsorption, the adsorbent's known weight in a volume of 100.00 cm^3 of the adsorbate of the desired concentration was agitated in 250 cm^3 stoppered conical flasks in a thermostated shaker at a speed of 200 strokes per minute. After pre-determined contact time, 10.00 cm^3 volume was pipetted out from each solution and centrifuged at 3000 rpm for 10 minutes. The supernatant was filtered using No.41 Whatman ashless filter paper. The filtrate was analyzed for residual adsorbate concentrations using the Air-acetylene flame of the atomic absorption spectrometer (Thermo scientific iCE 3000 series AAS equipped with robust flame, sample introduction system). Studies were done under ambient pH value except when investigating the effect of pH of the solution on metal ion adsorption by DBF. Each experiment was done triplicate.

Equation 1 was used to present the results as the removal efficiency or percentage removal:

$$\%\, removal = [\frac{C_o - C_t}{C_o}] \times 100 \qquad (1)$$

Where, C_0 is the initial adsorbate concentration in the solution, and C_t is the adsorbate concentration at time t in mg dm^{-3}.

Equation 2 was used to calculate the number of metal ions adsorbed by DBF.

$$q = \left[\frac{(C_0 - C_e)V}{W}\right] \qquad (2)$$

Where, q is the adsorption capacity (mg g^{-1}), C_e is the equilibrium concentration of the metal ions (mg dm^{-3}), V is the metal ion volume in the solution in dm^3, and W is the mass of adsorbent (g).

3. Results and Discussion

3.1. Characterization.

3.1.1. SEM analysis.

SEM micrographs were used to study the morphology of DBF, as shown in Figure 1. It indicates an uneven and irregular surface with tunnels like structures on it, enhancing the surface area and adsorption capacity of the adsorbent.

3.1.2. FTIR analysis of adsorbent.

FTIR analysis is a simple and easy method to determine the functional groups present in the DBF surface, identify the contribution of those functional groups in metal ion binding and the mechanisms involved in the adsorption process. FTIR spectrum recorded for native (pure) adsorbent is given in Figure 2. A comparison between the obtained FTIR spectrums before and after Cu(II) ions adsorption on to the adsorbent is given in Figure 3.

Absorption bands consisted of spectra are assigned based on structural properties and chemical components in plant cell walls and cuticles. A broad and strong absorption band gave between 3200-3600 cm^{-1} indicates the presence of exchangeable protons, which can be attributed to the stretching vibrations of –OH functional groups. The absorption band within the range 2900-2850 cm^{-1} can be assigned to C-H stretching vibrations by alkyl groups. Absorbance facilitated by carbonyl functional stretching of carboxylic, aldehyde, or ester

linkages (-C=O) gives at around 1730 cm^{-1}. The absorption band positioned around 1610 cm^{-1} can represent the characteristic amide frequencies. N-H bending vibration associated with amide groups is represented by the absorption band around 1515 cm^{-1}. The Weak absorption bands observed in the 1421-1373 cm^{-1} range are characteristics of CH_2 and CH_3 deformations. The absorption peak at 1243 cm^{-1} represents C-N stretching vibrations. A prominent peak at 1023 cm^{-1} indicates the stretching vibrations of –C-O-C and –OCH_3 groups in DBF.

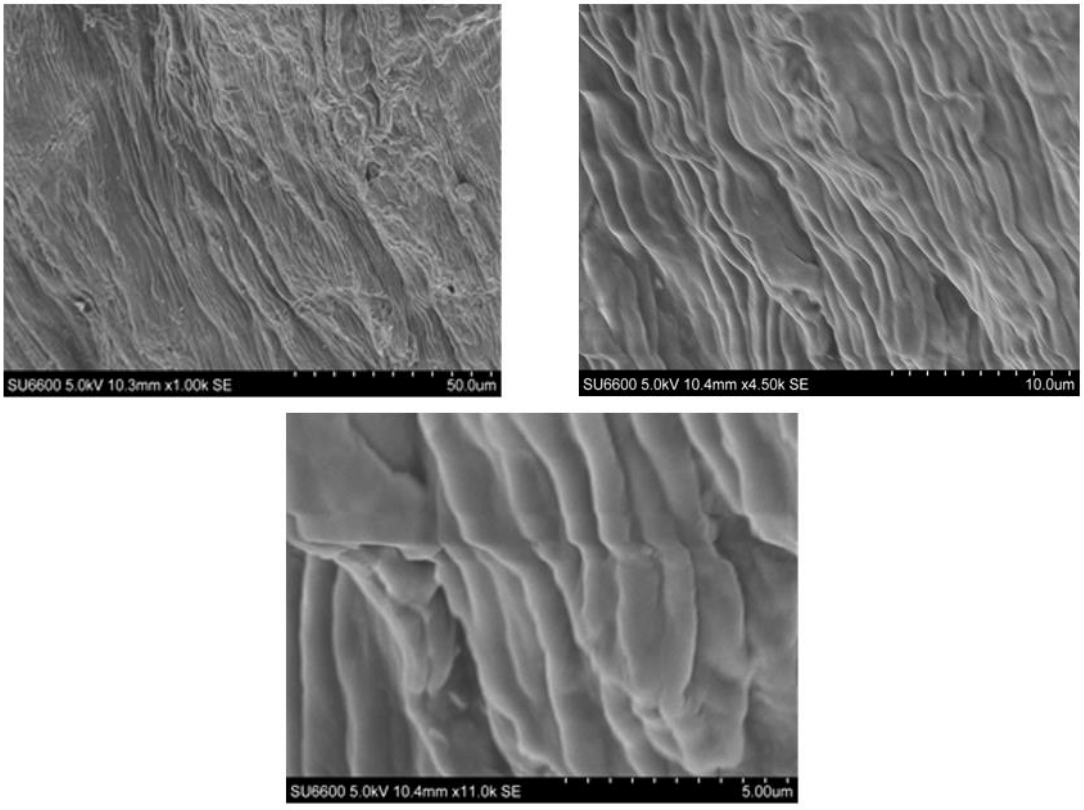

Figure 1. SEM images of untreated dried bael flowers.

According to Figure 3, a reduction in peak broadening and intensity can be observed in the peak around 3280 $cm^{-1,}$ indicating the concentration lowering in –OH groups after Cu(II) ions adsorption. A similar phenomenon can be seen with the peaks relating to –C-O, –C=O, and amide functional groups. Based on the results, it can be suggested that –OH, –C-O, –C=O, and amide groups on the adsorbent may be attributed to metal ion binding [23].

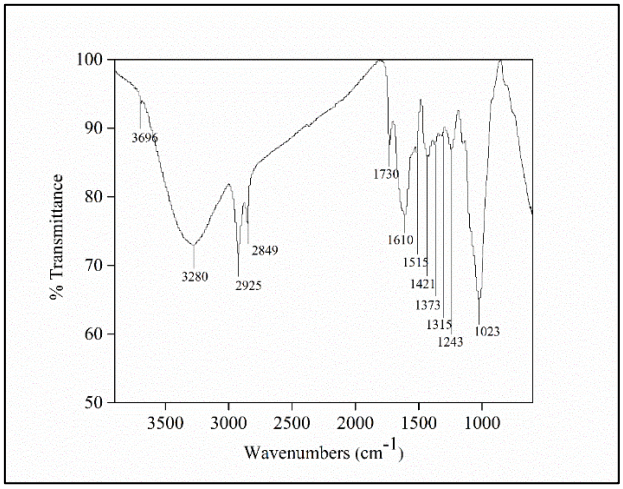

Figure 2. FTIR spectrum of untreated dried bael flowers at 30ºC.

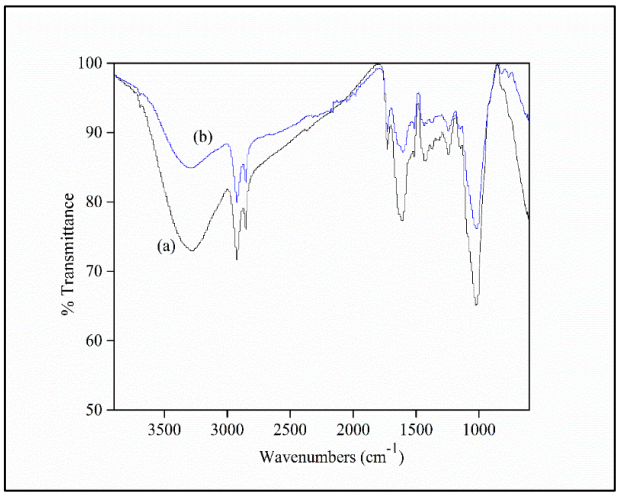

Figure 3. FTIR spectrum of (a) untreated dried bael flowers (b) Cu(II) adsorbed bael flowers at 30ºC.

3.2. Effect of contact time and adsorption kinetic studies.

Solutions obtained after agitating for specific periods with the adsorbent were analyzed for residual metal concentrations, as shown in Figure 4. As can be seen, the rate of Cu(II) adsorption initially shows an increasing trend with increasing contact time till the adsorption process reaches a state where the adsorbed metal ions come to a dynamic equilibrium with the number of metal ions desorbed from the adsorbent. The sharp increase in percentage removal within the first few minutes indicates that initially, plenty of readily accessible sites are available for the metal ions on the DBF surface [24].

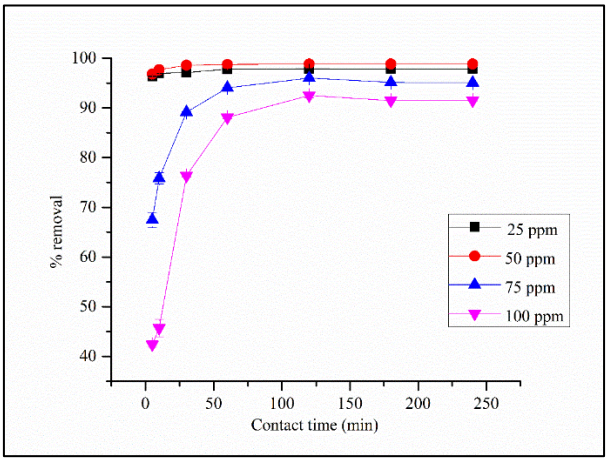

Figure 4. Effect of contact time on adsorption of Cu(II) ions onto dried bael flowers at various initial Cu (II) concentrations, 30 ºC, adsorbent dosage 0.500 g/100 ml, and particle size 250-500 µm.

It gradually decreased and reached equilibrium as most of the surface adsorption sites become occupied by metal ions. Amarasinghe and Williams also suggested a similar behavior for the removal of Cu(II) and Pb(II) by tea waste [25]. The system seems to reach an equilibrium around 120 minutes, which shows high efficiency in practical applications.

Kinetic models are important to explain the adsorption process's controlling mechanisms. They are useful to describe the target sorbate uptake rate[26]. The pseudo-second-order kinetic model was fitted with the experimental data giving squared correlation coefficient (R^2) values almost equal to unity. The calculated experimental q_e (equilibrium adsorption capacity) values were much closer to theoretical q_e values as shown in Table 1. This model, which is explained by Equation 3, is based on the assumption that the rate-limiting step is

chemisorption[27]. The kinetic data for the Cu(II) ions adsorption on to DBF is illustrated in Figure 5.

Experimental data were also fitted to the pseudo-first-order model, intraparticle diffusion model, and liquid film diffusion model given by Equation 4, Equation 5, and Equation 6, respectively. The kinetic parameters obtained from these models are given in Table 1. According to the results, these kinetic models showed a poor-fitting to Cu(II) ions adsorption on to DBF.

$$\frac{t}{q_t} = \frac{1}{k_2 q_e^2} + \frac{1}{q_e} t \quad (3)$$

$$\log(q_e - q_t) = \log q_e - \frac{k_1}{2.303} t \quad (4)$$

$$q_t = k_{id} t^{1/2} + C \quad (5)$$

$$ln(1 - F) = -k_{fd} t \quad (6)$$

Where, k_2 (g mg^{-1} min^{-1}) and k_1 (min^{-1}) are the rate constants for pseudo-second-order adsorption and pseudo-first-order adsorption respectively, q_t (mg g^{-1}) is the adsorbed solute amount at time t, q_e (mg g^{-1}) denotes the maximum adsorption capacity, and t (min) is the time. k_{id} (mg g^{-1} min$^{-1/2}$) is the intraparticle diffusion rate constant, and C (mg g^{-1}) is the intercept, which indicates the boundary layer thickness. F (q_t/q_e) is the fraction of solute adsorbed, k_{fd} (min^{-1}) is the rate constant of the film diffusion adsorption.

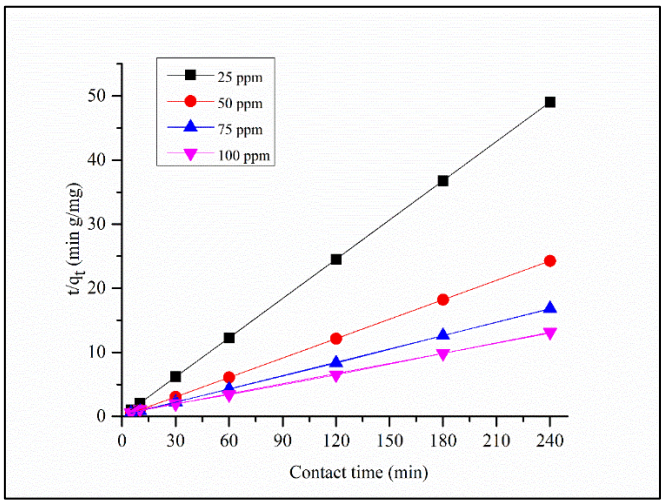

Figure 5. Pseudo-second-order plot for Cu(II) adsorption by dried bael flowers at 30 ºC, dosage 0.500 g/100 ml, and particle size 250-500 µm.

Table 1. Kinetic parameters of Cu(II) ions adsorption on to dried bael flowers at 30°C.

Conc. (ppm)	Pseudo-first- order			Pseudo-second-order			Intraparticle diffusion		Liquid film diffusion		Experim-ental qe (mg g^{-1})
	K_1 (min^1)	q_e (mg g^{-1})	R^2	K_2 (g mg^{-1} min^{-1})	q_e (mg g^{-1})	R^2	k_{id} (mg g^{-1} min$^{-1/2}$)	R^2	k_{fd} (min^{-1})	R^2	
25	0.02	0.05	0.875	1.77	4.82	0.998	0.01	0.760	0.01	0.875	4.82
50	-	-	-	-0.07	8.32	0.999	-0.03	0.165	-	-	8.38
75	0.01	2.03	0.774	0.04	16.42	0.999	0.26	0.699	0.01	0.774	16.41
100	0.02	6.47	0.867	0.01	19.49	0.999	0.75	0.747	0.02	0.867	19.04

3.3. Effect of initial metal ion concentration and isothermal adsorption studies.

Figure 6 illustrates the influence of initial metal ion concentration on metal ion removal. According to the results, the percentage removal of Cu(II) ions seems to reach a maximum

level (98.7%) when the initial metal concentration is around 50 ppm. Further enhancement in initial metal ion concentration caused a reduction in percentage removal values due to the saturation of binding sites on the adsorbent [28]. At lower initial metal ion concentrations, the concentration gradient between the solid and liquid phases is very low. Due to that reason, the generated driving force is not very strong; thus, the percentage removal values are comparatively low at lower initial metal ion concentrations [17].

To study the mechanism of Cu(II) ions uptake into the DBF, batch adsorption tests on isotherms were conducted at 30 ºC. Experimental data were fitted to the Langmuir, Freundlich, and Dubinin-Radushkevich (D-R) models represented by Equations 7, 8, and 9, respectively. The obtained results are summarized in Table 2.

$$\frac{C_e}{q_e} = \frac{1}{bq_m} + \frac{C_e}{q_m} \quad (7)$$

$$qe = K\,Ce^{1/n} \quad (8)$$

$$\ln q_e = \ln q_m - \beta\varepsilon^2 \quad (9)$$

$$\varepsilon = RT \ln\left(1 + \frac{1}{C_e}\right) \quad (10)$$

Where, C_e (mg dm^{-3}) is the equilibrium adsorbate concentration, q_e (mg g^{-1}) is the amount of Cu(II) ions adsorbed per unit mass of DBF at equilibrium, q_m (mg g^{-1}) is the maximum adsorption capacity regarding a monolayer coverage on DBF Surface and b is the Langmuir constant, 1/n and K are Freundlich adsorption isotherm constants, β (mol^2 J^{-2}) are the activity coefficient constant related to the mean free energy of adsorption, T (K) is the absolute temperature at equilibrium, ε is the D-R constant and R (J K^{-1} mol^{-1}) is the universal gas constant.

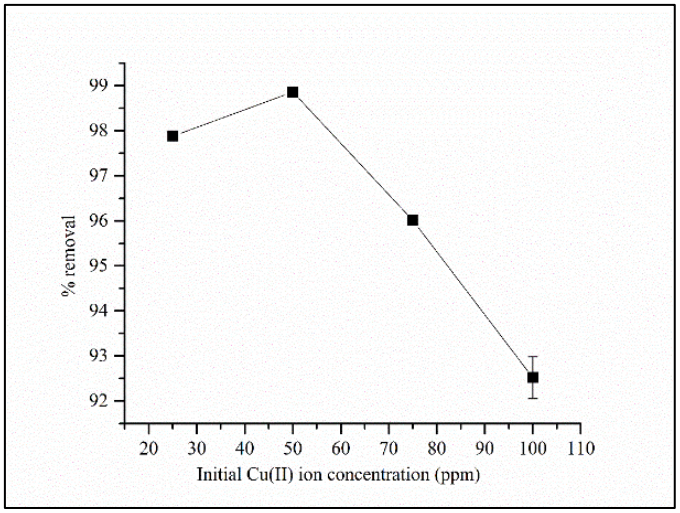

Figure 6. Effect of initial concentration on adsorption of Cu(II) ions onto dried bael flowers at 30ºC, adsorbent dosage 0.500 g/100 ml, and particle size 250-500 µm for 120 minutes contact time.

Table 2. Parameters obtained from Langmuir, Freundlich, and D-R isotherms at 30 ºC.

Langmuir isotherm			**Freundlich isotherm**			**D-R isotherm**		
b (dm^3 mg^{-1})	q_m (mg g^{-1})	R^2	K	1/n	R^2	qm (mg g^{-1})	β (mol^2 J^{-2})	R^2
0.69	23.14	0.974	8.53	0.45	0.857	18.82	0.16	0.911

According to Table 2, the Langmuir isotherm model fitted well with the experimental data compared to the other models (R^2 = 0.974), as shown in figure 7. The calculated maximum

adsorption capacity value was 23.14 mg g^{-1}. This indicates that the Cu(II) ions adsorption onto the DBF surface can be explained by the Langmuir isotherm model assumptions, which are, Cu(II) ions from a monolayer on the surface of DBF, adsorbent possesses active sites that are energetically equivalent and no interactions between adsorbed Cu(II) ions [29].

The adsorption behavior of metal ions onto DBF was further assessed by the separation factor, predicting whether a sorption system is favorable or unfavorable in a batch adsorption process. This dimensionless constant is given by Equation 11.

$$R_L = \frac{1}{1 + bC_0} \qquad (11)$$

Where C_0 (mg dm^{-3}) is the initial metal ion concentration. R_L values indicate whether the shape of the isotherm process is irreversible *(R_L=0)*, linear *(R_L=1)*, favorable *(0<R_L<1)*, or unfavorable *(R_L>1)*. The calculated R_L values corresponding to this adsorption process are given in Table 3. As seen in Table 3, all calculated R_L values lie within 0 and 1, which indicates the adsorption of Cu(II) ions onto DBF is favorable. Low R_L values obtained at higher Cu(II) concentrations indicate that adsorbate-adsorbent interactions become stronger at higher concentrations[30].

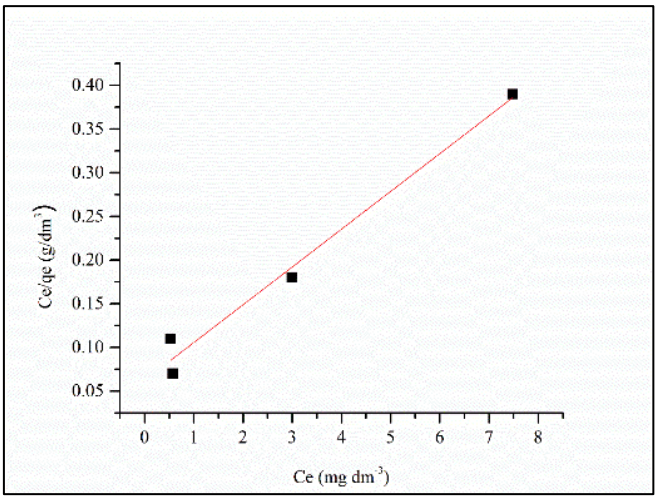

Figure 7. Langmuir isotherm plot for Cu(II) adsorption by dried bael flowers at 30ºC.

Table 3. R_L values were obtained for Cu(II) adsorption at 30 ºC for various initial concentrations.

Concentration (ppm)	25	50	75	100
R_L values	0.055	0.028	0.019	0.014

Comparison between the present study and the reported literature for Cu (II) ions adsorption is summarized in Table 4.

Table 4. Performance comparison of adsorbents for Cu(II) ion removal.

Adsorbent	**Adsorption capacity (mg/g)**	**Reference**
Raw wall nut shell modified by non-thermal plasma	39.4	[31]
Persimmon leaf bio-waste	19.42	[20]
Chemically modified marine algae	13.996	[32]
Alkali-treated coconut coir	7.86	[33]
Bottom ash of expired drugs incineration	13.335	[34]
Activated carbon prepared from olive branches	43.10	[35]
Sesame seed cake powder	4.24	[36]
Marine red algae biomass	47.62	[37]
Dried bael flowers	23.14	This study

According to the data summarized in Table 4, DBF possesses a reasonable capacity to adsorb Cu(II) ions from aqueous solutions. Therefore, DBF can be explored as a novel low-cost adsorbent for wastewater treatment in future applications.

3.4. Effect of temperature and adsorption thermodynamic studies.

The effect of temperature on the Cu(II) ions adsorption process was investigated in the 20 ºC - 60 ºC temperature range (Figure 8). At 120 minutes of contact time, the percentage removal of Cu(II) decreases from 98.8% to 95% when temperature increase from 20 ºC to 60 ºC suggesting the adsorption process is exothermic[38]. An increase in temperature probably weakens the adsorptive forces between the metal ions and active sites on DBF. The metal ions desorb back to the solution resulting in low metal adsorption. This indicates that the physisorption mechanism takes place during the adsorption process.

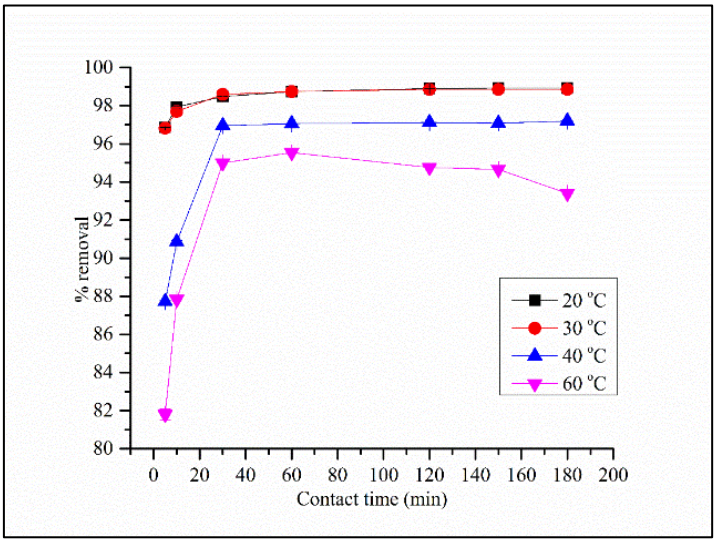

Figure 8. Effect of temperature on percentage removal of Cu(II) ions by dried bael flowers at 50 ppm initial Cu (II) concentration, 30 ºC, 0.500 g/100 ml adsorbent dosage and particle size 250-500 µm.

The equilibrium constants and Gibbs free energy changes for the Cu(II) ions adsorption on to DBF were calculated using Equation 12 and Equation 13, respectively[39].

$$K_o = \frac{C_s}{C_l} \quad (12)$$

$$\Delta G^0 = -RTlnK_0 \quad (13)$$

Where K_0 is the equilibrium constant of the adsorption process at a certain temperature. C_s (mg dm^{-3}) and C_l (mg dm^{-3}) are the solid phase concentration and liquid phase concentration of adsorbate at equilibrium. The obtained results are summarized in Table 5.

The negative ΔG values confirm that the adsorption of Cu(II) ions on the DBF surface is spontaneous. When the temperature increases from 20 ºC to 60 ºC, the negativity of ΔG values decreases. A decrease in ΔG values with increasing temperature implies that the adsorption process's spontaneity decreases with increasing temperature, resulting in the weakening of bonds formed between the active sites and metal ions.

The enthalpy and entropy changes for the adsorption process were calculated by fitting the obtained data into Equation 14, as shown in Figure 9. The results are given in Table 5.

The positive slope obtained from the Van Hoff plot and the negative ΔH value confirm that the adsorption process is exothermic in nature. The negative ΔS value indicates the decrease in the randomness of metal ions at the solid-liquid interface of the adsorbent. These findings are in agreement with some previous studies[40, 41].

$$\log K_o = \frac{\Delta S}{2.303\,R} - \frac{\Delta H}{2.303\,RT} \quad (14)$$

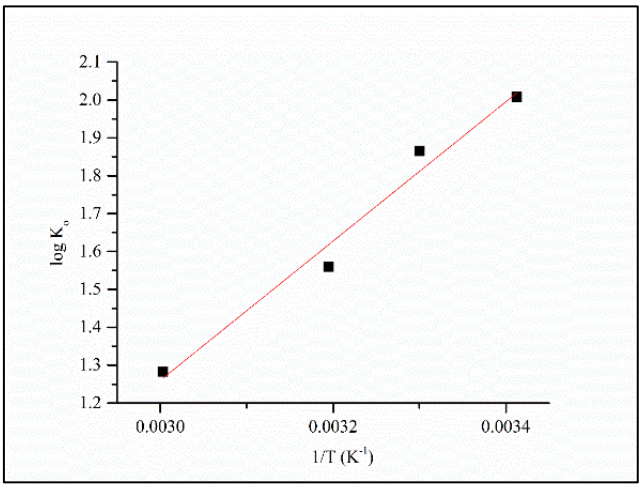

Figure 9. The plot of *log K_0* versus *1/T* for estimating thermodynamic parameters for the Cu(II) adsorption process.

Table 5. Thermodynamic parameters for Cu(II) ions adsorption on to Dried bael flowers.

Temperature (K)	Equilibrium constant *(K_0)*	ΔG (kJ mol^{-1})	ΔH (kJ mol^{-1})	ΔS(kJ mol^{-1} K^{-1})
293	101.82	-11.26		
303	73.32	-10.82	- 35.18	- 0.081
313	36.25	-9.34		
333	19.16	-8.18		

3.5. Effect of pH of the solution.

The pH optimization study was done for Cu(II) ions adsorption on the DBF within 2 - 8 pH ranges. As seen in Figure 10, Cu(II) ions removal showed a positive correlation with the medium's pH increment. It became constant around pH 4 – 7, resulting in approximately 98% removal.

pH is critically linked with the degree of ionization and the charge on the adsorbent surface. The functional groups on the adsorbent surface, responsible for metal binding, get protonated at low pH values [42]. Furthermore, at lower pH, H^+ ions compete with metal ions for the adsorbent's active sites. The gradual increase in Cu(II) ions percentage adsorption with pH increment possibly can be related to the de-protonation of the binding sites making them available for metal ion binding while reducing the competition between adsorbate (Cu (II) ions) and protons.

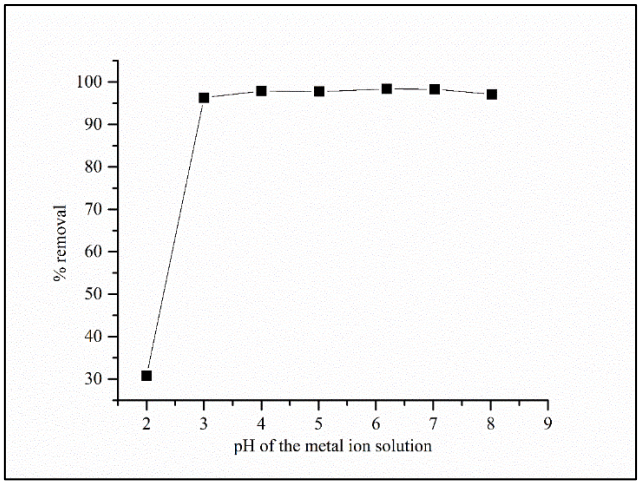

Figure 10. Effect of pH on percentage removal of Cu(II) ions by DBF at 50 ppm initial concentrations, 30 ºC, adsorbent dosage 0.500 g/100 ml, and particle size 250-500 µm for 120 minutes contact time.

3.6. Effect of adsorbent dosage.

The effect of biomass dosage on metal adsorption is shown in Figure 11. The percentage removal of metal ions increased with the adsorbent dosage. Above 0.5 g/100 ml dosages, the percentage of removal increment was low. When increasing the adsorbent dosage, more adsorption sites are available for the metal ion binding. The percentage of removal values tend to increase[43]. The binding sites remain unsaturated at higher adsorption dosages (above 0.5 g/100 ml) due to overlapping and aggregation [44].

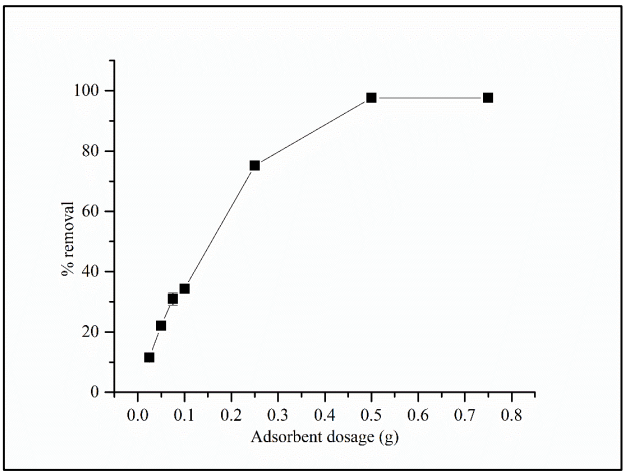

Figure 11. Effect of adsorbent dosage on percentage removal of Cu(II) ions by dried bael flowers at 50 ppm initial concentration,100 ml, 30 ºC, and particle size 250-500 µm for 120 minutes contact time.

4. Conclusions

Dried Beal flowers were found to be a promising low-cost alternative adsorbent for the adsorptive removal of Cu(II) ions from aqueous solutions. The SEM studies indicated that adsorbent has an uneven and irregular surface structure with tubular pores. FTIR analysis indicated the possession of various functional groups such as hydroxyl, C-O, -C=O, and amide groups, which might be participated in metal removal. The adsorption process was dependent upon the tested operating parameters: pH of the medium, contact time, initial metal ion concentration, adsorbent dosage, and temperature. The maximum percentage removal of 98.7% was observed at 50 ppm initial metal ion concentration, 120 minutes contact time, 0.5 g adsorbent dosage in 100 ml Cu(II) ion solution, 30 ºC temperature, and pH of 7. Langmuir isotherm model and the pseudo-second-order kinetic model fitted well with the experimental data. The obtained maximum adsorption capacity is 23.14 mg g^{-1}. Calculated thermodynamic parameters (ΔG, ΔH, ΔS) suggest the adsorption process of Cu(II) is spontaneous and exothermic. Both physisorption and chemisorption processes seem to take place during the adsorption process. Therefore dried bael flowers can be applied as an effective and economical natural adsorbent to treat wastewater containing Cu(II) ions.

Funding

The study was funded by the University of Sri Jayewardenepura, Sri Lanka.

Acknowledgments

The authors would like to thank the Sri Lanka Institute of Nanotechnology (SLINTEC), for technical support in SEM work.

Conflicts of Interest

The authors declare no conflict of interest.

References

1. Putra, W.; Kamari, A.; Najiah, S.; Yusoff, M.; Ishak, C.; Mohamed, A.; Hashim, N.; Isa, I.; Putra, W. Biosorption of Cu(II), Pb(II) and Zn(II) Ions from Aqueous Solutions Using Selected Waste Materials: Adsorption and Characterisation Studies. *Journal of Encapsulation and Adsorption Sciences* **2014**, *4*, 25-35, http://dx.doi.org/10.4236/jeas.2014.41004.
2. Llanos, R.M.; Mercer, J.F. The molecular basis of copper homeostasis copper-related disorders. *DNA and cell biology* **2002**, *21*, 259-270, http://doi.org/10.1089/104454902753759681.
3. Singha, B.; Das, S.K. Adsorptive removal of Cu(II) from aqueous solution and industrial effluent using natural/agricultural wastes. *Colloids Surf B Biointerfaces* **2013**, *107*, 97-106, http://dx.doi.org/10.1016/j.colsurfb.2013.01.060.
4. Zhu, B.; Fan, T.; Zhang, D. Adsorption of copper ions from aqueous solution by citric acid modified soybean straw. *Journal of hazardous materials* **2008**, *153*, 300-308, https://doi.org/10.1016/j.jhazmat.2007.08.050.
5. Mohiuddin, K.M.O.Y.Z.; H.M.; Otomo, K.; Shikazono, N. Heavy metals contamination in water and sediments of an urban river in a developing country. *International journal of Environmental Science and Technology* **2011,** 723-736. https://doi.org/10.1007/bf03326257.
6. Varol, M.; Şen, B. Assessment of nutrient and heavy metal contamination in surface water and sediments of the upper Tigris River, Turkey. *Catena* **2012**, *92*, 1-10, https://doi.org/10.1016/j.catena.2011.11.011.
7. Petrov, O.; Petrichenko, S.; Yushchishina, A.; Mitryasova, O.; Pohrebennyk, V. Electrospark Method in Galvanic Wastewater Treatment for Heavy Metal Removal. *Applied Sciences* **2020**, *10*, https://doi.org/10.3390/app10155148.
8. Beiramzadeh, Z.; Baqersad, M.; Aghababaei, M. Application of the response surface methodology (RSM) in heavy metal removal from real power plant wastewater using electrocoagulation. *European Journal of Environmental and Civil Engineering* **2019**, 1-19, https://doi.org/10.1080/19648189.2019.1640139.
9. Lin, S.; Li, Q.; Zhong, Y.; Li, J.; Zhao, X.; Wang, M.; Zhao, G.; Pan, J.; Zhu, H. Cross-Linked Double Network Graphene Oxide/Polymer Composites for Efficient Coagulation-Flocculation. *Global Challenges*, **2020**, *4*.
10. Zhao, Z.; An, H.; Lin, J.; Feng, M.; Murugadoss, V.; Ding, T.; Liu, H.; Shao, Q.; Mai, X.; Wang, N.; Gu, H.; Angaiah, S.; Guo, Z. Progress on the photocatalytic reduction removal of chromium contamination. *The Chemical Record* **2019**, *19*, 873-882, https://doi.org/10.1002/tcr.201800153.
11. Dong, Q.; Guo, X.; Huang, X.; Liu, L.; Tallon, R.; Taylor, B.; Chen, J. Selective removal of lead ions through capacitive deionization: Role of ion-exchange membrane. *Chemical Engineering Journal* **2019**, *361*, 1535-1542, https://doi.org/10.1016/j.cej.2018.10.208.
12. Efome, J.E.; Rana, D.; Matsuura, T.; Lan, C.Q. Effects of operating parameters and coexisting ions on the efficiency of heavy metal ions removal by nano-fibrous metal-organic framework membrane filtration process. *Science of The Total Environment* **2019**, *674*, 355-362, https://doi.org/10.1016/j.scitotenv.2019.04.187.
13. Vilvanathan, S.; Shanthakumar, S. Ni2+ and Co2+ adsorption using Tectona grandis biochar: kinetics, equilibrium and desorption studies. *Environmental Technology* **2017**, *39*, 464-478, http://dx.doi.org/10.1080/09593330.2017.1304454.
14. Bayuo, J.; Pelig-Ba, K.B.; Abukari, M.A. Adsorptive removal of chromium(VI) from aqueous solution unto groundnut shell. *Applied Water Science* **2019**, *9*, https://doi.org/10.1007/s13201-019-0987-8.
15. Grenni, P.; Barra Caracciolo, A.; Mariani, L.; Cardoni, M.; Riccucci, C.; Elhaes, H.; Ibrahim, M.A. Effectiveness of a new green technology for metal removal from contaminated water. *Microchemical Journal* **2019**, *147*, 1010-1020, https://doi.org/10.1016/j.microc.2019.04.026.
16. Ranaweera, K.H.; Godakumbura, P.I.; Perera, B.A. Adsorptive removal of Co(II) in aqueous solutions using clearing nut seed powder. *Heliyon* **2020**, *6*, https://doi.org/10.1016/j.heliyon.2020.e03684.
17. Mohamed, H.S.; Soliman, N.K.; Abdelrheem, D.A.; Ramadan, A.A.; Elghandour, A.H.; Ahmed, S.A.Adsorption of Cd^{2+} and Cr^{3+} ions from aqueous solutions by using residue of Padina gymnospora waste as promising low-cost adsorbent. *Heliyon* **2019**, *5*, https://doi.org/10.1016/j.heliyon.2019.e01287.
18. Banerjee, M.; Basu, R.k.; Das, S.K. Adsorptive removal of Cu(II) by pistachio shell: Isotherm study, kinetic modelling and scale-up designing — continuous mode. *Environmental Technology & Innovation* **2019**, *15*, https://doi.org/10.1016/j.eti.2019.100419.
19. Gaur, N.; Kukreja, A.; Yadav, M.; Tiwari, A. Adsorptive removal of lead and arsenic from aqueous solution using soya bean as a novel biosorbent: equilibrium isotherm and thermal stability studies. *Applied Water Science* **2018**, *8*, https://doi.org/10.1007/s13201-018-0743-5.
20. Lee, S.-Y.; Choi, H.-J. Persimmon leaf bio-waste for adsorptive removal of heavy metals from aqueous solution. *Journal of Environmental Management* **2018**, *209*, 382-392, https://doi.org/10.1016/j.jenvman.2017.12.080.

21. Chakravarty, S.; Mohanty, A.; Sudha, T.N.; Upadhyay, A.K.; Konar, J.; Sircar, J.K.; Madhukar, A.; Gupta, K.K. Removal of Pb(II) ions from aqueous solution by adsorption using bael leaves (Aegle marmelos). *Journal of Hazardous Materials* **2010**, *173*, 502-509, https://doi.org/10.1016/j.jhazmat.2009.08.113.
22. Virendra, T.; Rashmi, S.; Pandey, A. Aegle marmelos: pharmacological, medicinal importance and conservation in India. *Journal of Experimental Zoology, India* **2018**, *21* 11-18, https://doi.org/10.13140/RG.2.2.17267.84001.
23. Thirumavalavan, M.; Lai, Y.-L.; Lee, J.-F. Fourier Transform Infrared Spectroscopic Analysis of Fruit Peels before and after the Adsorption of Heavy Metal Ions from Aqueous Solution. *Journal of Chemical & Engineering Data* **2011**, *56*, 2249-2255, https://doi.org/10.1021/je101262w.
24. Kumar, P.S.; Vincent, C.; Kirthika, K.; Kumar, K.S. Kinetics and equilibrium studies of Pb2+ in removal from aqueous solutions by use of nano-silversol-coated activated carbon. *J Brazilian Journal of Chemical Engineering* **2010**, *27*, 339-346, https://doi.org/10.1590/S0104-66322010000200012
25. Amarasinghe, B.M.W.P.K.; Williams, R.A. Tea waste as a low cost adsorbent for the removal of Cu and Pb from wastewater. *Chemical Engineering Journal* **2007**, *132*, 299-309, https://doi.org/10.1016/j.cej.2007.01.016.
26. Wang, B.; Bai, Z.; Jiang, H.; Prinsen, P.; Luque, R.; Zhao, S.; Xuan, J. Selective heavy metal removal and water purification by microfluidically-generated chitosan microspheres: Characteristics, modeling and application. *Journal of Hazardous Materials* **2019**, *364*, 192-205, https://doi.org/10.1016/j.jhazmat.2018.10.024.
27. Ho, Y.-S. Review of second-order models for adsorption systems. *Journal of Hazardous Materials* **2006**, *136*, 681-689, https://doi.org/10.1016/j.jhazmat.2005.12.043.
28. El-Tawil, R.S.; El-Wakeel, S.T.; Abdel-Ghany, A.E.; Abuzeid, H.A.M.; Selim, K.A.; Hashem, A.M. Silver/quartz nanocomposite as an adsorbent for removal of mercury (II) ions from aqueous solutions. *Heliyon* **2019**, *5*, https://doi.org/10.1016/j.heliyon.2019.e02415.
29. Wong, Y.C.; Szeto, Y.S.; Cheung, W.H.; McKay, G. Equilibrium Studies for Acid Dye Adsorption onto Chitosan. *Langmuir* **2003**, *19*, 7888-7894, https://doi.org/10.1021/la030064y.
30. Jayaram, K.; Murthy, I.Y.L.N.; Lalhruaitluanga, H.; Prasad, M.N.V. Biosorption of lead from aqueous solution by seed powder of Strychnos potatorum L. *Colloids and Surfaces B: Biointerfaces* **2009**, *71*, 248-254, https://doi.org/10.1016/j.colsurfb.2009.02.016.
31. Wu, L.; Shang, Z.; Chen, S.; Tu, J.; Kobayashi, N.; Li, Z. Raw walnut shell modified by non-thermal plasma in ultrafine water mist for adsorptive removal of Cu(ii) from aqueous solution. *RSC Advances* **2018**, *8*, 21993-22003, https://doi.org/10.1039/C8RA03271H.
32. Foroutan, R.; Esmaeili, H.; Abbasi, M.; Rezakazemi, M.; Mesbah, M. Adsorption behavior of Cu(II) and Co(II) using chemically modified marine algae. *Environmental Technology* **2018**, *39*, 2792-2800, https://doi.org/10.1080/09593330.2017.1365946.
33. Asim, N.; Amin, M.H.; Samsudin, N.A.; Badiei, M.; Razali, H.; Akhtaruzzaman, M.; Amin, N.; Sopian, K. Development of effective and sustainable adsorbent biomaterial from an agricultural waste material: Cu(II) removal. *Materials Chemistry and Physics* **2020**, *249*, https://doi.org/10.1016/j.matchemphys.2020.123128.
34. Benzaoui, T.; Selatnia, A.; Djabali, D. Adsorption of copper (II) ions from aqueous solution using bottom ash of expired drugs incineration. *Adsorption Science & Technology* **2017**, *36*, 114-129, https://doi.org/10.1177/0263617416685099.
35. Alkherraz, A.M.; Ali, A.K.; Elsherif, K.M. Removal of Pb (II), Zn (II), Cu (II) and Cd (II) from aqueous solutions by adsorption onto olive branches activated carbon: equilibrium and thermodynamic studies. *Chem. Int.* **2020**, *6*, 11-20, https://doi.org/10.5281/zenodo.2579465.
36. Pavan Kumar, G.V.S.R.; Malla, K.A.; Yerra, B.; Srinivasa Rao, K. Removal of Cu(II) using three low-cost adsorbents and prediction of adsorption using artificial neural networks. *Applied Water Science* **2019**, *9*, https://doi.org/10.1007/s13201-019-0924-x.
37. Lucaci, A.R.; Bulgariu, D.; Popescu, M.-C.; Bulgariu, L. Adsorption of Cu(II) Ions on Adsorbent Materials Obtained from Marine Red Algae Callithamnion corymbosum sp. *Water* **2020**, *12*, https://doi.org/10.3390/w12020372.
38. Mahindrakar, K.V.; Rathod, V.K. Utilization of banana peels for removal of strontium (II) from water. *Environmental Technology & Innovation* **2018**, *11*, 371-383, https://doi.org/10.1016/j.eti.2018.06.015.
39. Sherlala, A.I.A.; Raman, A.A.A.; Bello, M.M.; Buthiyappan, A. Adsorption of arsenic using chitosan magnetic graphene oxide nanocomposite. *Journal of Environmental Management* **2019**, *246*, 547-556, https://doi.org/10.1016/j.jenvman.2019.05.117.
40. Maji, S.; Ghosh, A.; Gupta, K.; Ghosh, A.; Ghorai, U.; Santra, A.; Sasikumar, P.; Ghosh, U.C. Efficiency evaluation of arsenic(III) adsorption of novel graphene oxide@iron-aluminium oxide composite for the contaminated water purification. *Separation and Purification Technology* **2018**, *197*, 388-400, https://doi.org/10.1016/j.seppur.2018.01.021.
41. Senthil Kumar, P.; Sai Deepthi, A.S.L.; Bharani, R.; Prabhakaran, C. Adsorption of Cu(II), Cd(II) and Ni(II) ions from aqueous solution by unmodified Strychnos potatorum seeds. *European Journal of Environmental and Civil Engineering* **2013**, *17*, 293-314, https://doi.org/10.1080/19648189.2013.785983.

42. Deng, L.; Su, Y.; Su, H.; Wang, X.; Zhu, X. Sorption and desorption of lead (II) from wastewater by green algae Cladophora fascicularis. *Journal of Hazardous Materials* **2007**, *143*, 220-225, https://doi.org/10.1016/j.jhazmat.2006.09.009.
43. Zhai, L.; Bai, Z.; Zhu, Y.; Wang, B.; Luo, W. Fabrication of chitosan microspheres for efficient adsorption of methyl orange. *Chinese Journal of Chemical Engineering* **2018**, *26*, 657-666, https://doi.org/10.1016/j.cjche.2017.08.015.
44. Sarkar, S.; Sarkar, M. Ultrasound assisted batch operation for the adsorption of hexavalent chromium onto engineered nanobiocomposite. *Heliyon* **2019**, *5*, https://doi.org/10.1016/j.heliyon.2019.e01491.